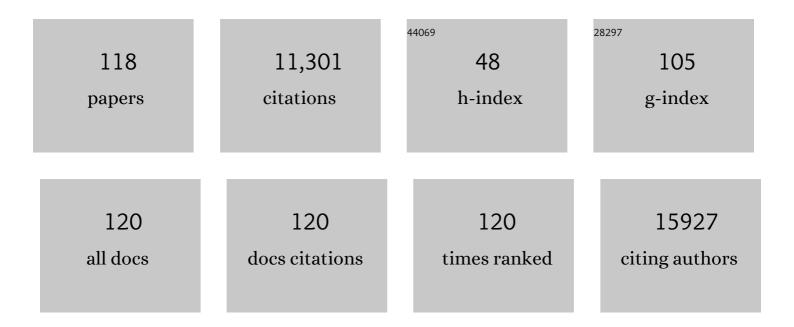
Dehong Hu

List of Publications by Year in descending order

Source: https://exaly.com/author-pdf/4298626/publications.pdf Version: 2024-02-01



DEHONG HU

#	Article	IF	CITATIONS
1	Impacts of The Wetland Sedge Carex aquatilis on Microbial Community and Methane Metabolisms. Plant and Soil, 2022, 471, 491.	3.7	2
2	Expression Patterns of Energy-Related Genes in Single Cells Uncover Key Isoforms and Enzymes That Gain Priority Under Nanoparticle-Induced Stress. ACS Nano, 2022, 16, 7197-7209.	14.6	3
3	Hydroporphyrin-Doped Near-Infrared-Emitting Polymer Dots for Cellular Fluorescence Imaging. ACS Applied Materials & Interfaces, 2022, 14, 20790-20801.	8.0	10
4	Metabolic Interactions between <i>Brachypodium</i> and Pseudomonas fluorescens under Controlled Iron-Limited Conditions. MSystems, 2021, 6, .	3.8	13
5	Single Molecule–Based fliFISH Validates Radial and Heterogeneous Gene Expression Patterns in Pancreatic Islet β-Cells. Diabetes, 2021, 70, 1117-1122.	0.6	6
6	Microbe-Encapsulated Silica Gel Biosorbents for Selective Extraction of Scandium from Coal Byproducts. Environmental Science & Technology, 2021, 55, 6320-6328.	10.0	12
7	High Throughput Mapping of Single Molecules' Redox Potentials on Electrode. Analytical Chemistry, 2021, 93, 8864-8871.	6.5	5
8	A Polymer-in-Salt Electrolyte with Enhanced Oxidative Stability for Lithium Metal Polymer Batteries. ACS Applied Materials & Interfaces, 2021, 13, 31583-31593.	8.0	28
9	Colloidal immobilized protein based on stable colloid of TiO nanoparticles at neutral pH for protein microarray. Colloids and Interface Science Communications, 2021, 43, 100440.	4.1	0
10	Counting mRNA Copies in Intact Bacterial Cells by Fluctuation Localization Imaging-Based Fluorescence In Situ Hybridization (fliFISH). Methods in Molecular Biology, 2021, 2246, 237-247.	0.9	3
11	Bridging Hydrometallurgy and Biochemistry: A Protein-Based Process for Recovery and Separation of Rare Earth Elements. ACS Central Science, 2021, 7, 1798-1808.	11.3	71
12	High-throughput and high-efficiency sample preparation for single-cell proteomics using a nested nanowell chip. Nature Communications, 2021, 12, 6246.	12.8	76
13	Preferential interactions of primary amine-terminated quantum dots with membrane domain boundaries and lipid rafts revealed with nanometer resolution. Environmental Science: Nano, 2020, 7, 149-161.	4.3	12
14	Correlative surface imaging reveals chemical signatures for bacterial hotspots on plant roots. Analyst, The, 2020, 145, 393-401.	3.5	15
15	Chemical plasticity in the fine root construct of <i>Quercus</i> spp. varies with root order and drought. New Phytologist, 2020, 228, 1835-1851.	7.3	20
16	Polystyrene nano- and microplastic accumulation at Arabidopsis and wheat root cap cells, but no evidence for uptake into roots. Environmental Science: Nano, 2020, 7, 1942-1953.	4.3	102
17	Genetic and metabolic links between the murine microbiome and memory. Microbiome, 2020, 8, 53.	11.1	56
18	Fluorescence in situ mRNA hybridization for gene expression detection in a wood decay fungus. International Biodeterioration and Biodegradation, 2019, 143, 104731.	3.9	2

Dehong Hu

#	Article	IF	CITATIONS
19	On Modeling Ensemble Transport of Metal Reducing Motile Bacteria. Scientific Reports, 2019, 9, 14638.	3.3	2
20	Quantitative Mapping of Oxidative Stress Response to Lithium Cobalt Oxide Nanoparticles in Single Cells Using Multiplexed <i>in Situ</i> Gene Expression Analysis. Nano Letters, 2019, 19, 1990-1997.	9.1	25
21	Stable Acinar Progenitor Cell Model Identifies Treacle-Dependent Radioresistance. Radiation Research, 2019, 192, 135.	1.5	4
22	Stability of polymeric separators in lithium metal batteries in a low voltage environment. Journal of Materials Chemistry A, 2018, 6, 5006-5015.	10.3	31
23	Fluctuation localization imaging-based fluorescence in situ hybridization (fliFISH) for accurate detection and counting of RNA copies in single cells. Nucleic Acids Research, 2018, 46, e7-e7.	14.5	31
24	Tumor Retention of Enzyme-Responsive Pt(II) Drug-Loaded Nanoparticles Imaged by Nanoscale Secondary Ion Mass Spectrometry and Fluorescence Microscopy. ACS Central Science, 2018, 4, 1477-1484.	11.3	39
25	Lipid Corona Formation from Nanoparticle Interactions with Bilayers. CheM, 2018, 4, 2709-2723.	11.7	46
26	Stable cycling of high-voltage lithium metal batteries in ether electrolytes. Nature Energy, 2018, 3, 739-746.	39.5	767
27	Controlling the structure and ferroic properties of strained epitaxial NiTiO3 thin films on sapphire by post-deposition annealing. Thin Solid Films, 2018, 662, 47-53.	1.8	3
28	Mutations That Alter the Bacterial Cell Envelope Increase Lipid Production. MBio, 2017, 8, .	4.1	10
29	Coupled Lattice Polarization and Ferromagnetism in Multiferroic NiTiO ₃ Thin Films. ACS Applied Materials & Interfaces, 2017, 9, 21879-21890.	8.0	18
30	Multimodal hyperspectral optical microscopy. Chemical Physics, 2017, 498-499, 25-32.	1.9	7
31	Multiple-targeted graphene-based nanocarrier for intracellular imaging of mRNAs. Analytica Chimica Acta, 2017, 983, 1-8.	5.4	27
32	A Protocol for Electrochemical Evaluations and State of Charge Diagnostics of a Symmetric Organic Redox Flow Battery. Journal of Visualized Experiments, 2017, , .	0.3	1
33	Organismal and spatial partitioning of energy and macronutrient transformations within a hypersaline mat. FEMS Microbiology Ecology, 2017, 93, .	2.7	23
34	Fluorescence Based Characterization of Calcium Sensitizer Action on the Troponin Complex. Chemical Biology and Drug Design, 2016, 87, 171-181.	3.2	9
35	Polyvinylpyrrolidone-induced anisotropic growth of gold nanoprisms in plasmon-driven synthesis. Nature Materials, 2016, 15, 889-895.	27.5	239
36	Cellular Delivery of Nanoparticles Revealed with Combined Optical and Isotopic Nanoscopy. ACS Nano, 2016, 10, 4046-4054.	14.6	36

ДЕНОИС НИ

#	Article	IF	CITATIONS
37	A symmetric organic-based nonaqueous redox flow battery and its state of charge diagnostics by FTIR. Journal of Materials Chemistry A, 2016, 4, 5448-5456.	10.3	167
38	Localizing gene regulation reveals a staggered wood decay mechanism for the brown rot fungus <i>Postia placenta</i> . Proceedings of the National Academy of Sciences of the United States of America, 2016, 113, 10968-10973.	7.1	160
39	Grain growth of nanocrystalline 3C-SiC under Au ion irradiation at elevated temperatures. Journal Physics D: Applied Physics, 2016, 49, 035304.	2.8	3
40	Cells Respond to Distinct Nanoparticle Properties with Multiple Strategies As Revealed by Single-Cell RNA-Seq. ACS Nano, 2016, 10, 10173-10185.	14.6	21
41	The information content in single-molecule Raman nanoscopy. Advances in Physics: X, 2016, 1, 35-54.	4.1	8
42	Multi-omics analysis reveals regulators of the response to nitrogen limitation in Yarrowia lipolytica. BMC Genomics, 2016, 17, 138.	2.8	62
43	Antigen Binding and Site-Directed Labeling of Biosilica-Immobilized Fusion Proteins Expressed in Diatoms. ACS Synthetic Biology, 2016, 5, 193-199.	3.8	15
44	Formation of supported lipid bilayers containing phase-segregated domains and their interaction with gold nanoparticles. Environmental Science: Nano, 2016, 3, 45-55.	4.3	68
45	Swimming Motility ReducesAzotobacter vinelandiiDeposition to Silica Surfaces. Journal of Environmental Quality, 2015, 44, 1366-1375.	2.0	6
46	Strain-Dependence of the Structure and Ferroic Properties of Epitaxial NiTiO ₃ Thin Films Grown on Different Substrates. Advances in Condensed Matter Physics, 2015, 2015, 1-9.	1.1	7
47	Alexa Fluor-Labeled Fluorescent Cellulose Nanocrystals for Bioimaging Solid Cellulose in Spatially Structured Microenvironments. Bioconjugate Chemistry, 2015, 26, 593-601.	3.6	52
48	Shifts in oxidation states of cerium oxide nanoparticles detected inside intact hydrated cells and organelles. Biomaterials, 2015, 62, 147-154.	11.4	52
49	Argon Cluster Sputtering Source for ToF-SIMS Depth Profiling of Insulating Materials: High Sputter Rate and Accurate Interfacial Information. Journal of the American Society for Mass Spectrometry, 2015, 26, 1283-1290.	2.8	24
50	A fundamental study on the [(μ-Cl) ₃ Mg ₂ (THF) ₆] ⁺ dimer electrolytes for rechargeable Mg batteries. Chemical Communications, 2015, 51, 2312-2315.	4.1	53
51	Lipopolysaccharide Density and Structure Govern the Extent and Distance of Nanoparticle Interaction with Actual and Model Bacterial Outer Membranes. Environmental Science & Technology, 2015, 49, 10642-10650.	10.0	103
52	Strain-dependence of the structure and ferroic properties of epitaxial Ni1â^'xTi1â^'yO3 thin films grown on sapphire substrates. Thin Solid Films, 2015, 578, 113-123.	1.8	7
53	Intracellular accumulation dynamics and fate of zinc ions in alveolar epithelial cells exposed to airborne ZnO nanoparticles at the air–liquid interface. Nanotoxicology, 2015, 9, 9-22.	3.0	51
54	A Specific Nucleophilic Ring-Opening Reaction of Aziridines as a Unique Platform for the Construction of Hydrogen Polysulfides Sensors. Organic Letters, 2015, 17, 2776-2779.	4.6	83

ДЕНОИС НИ

#	Article	IF	CITATIONS
55	Ultrafast Imaging of Surface Plasmons Propagating on a Gold Surface. Nano Letters, 2015, 15, 3472-3478.	9.1	69
56	Tip-Enhanced Raman Nanographs: Mapping Topography and Local Electric Fields. Nano Letters, 2015, 15, 2385-2390.	9.1	26
57	Direct Probes of 4 nm Diameter Gold Nanoparticles Interacting with Supported Lipid Bilayers. Journal of Physical Chemistry C, 2015, 119, 534-546.	3.1	77
58	Phototrophic biofilm assembly in microbial-mat-derived unicyanobacterial consortia: model systems for the study of autotroph-heterotroph interactions. Frontiers in Microbiology, 2014, 5, 109.	3.5	97
59	Electric field enhancement in a self-assembled 2D array of silver nanospheres. Journal of Chemical Physics, 2014, 141, 214308.	3.0	20
60	Frequency-Resolved Nanoscale Chemical Imaging of 4,4′-Dimercaptostilbene on Silver. Journal of Physical Chemistry C, 2014, 118, 27525-27530.	3.1	9
61	Facile method to stain the bacterial cell surface for super-resolution fluorescence microscopy. Analyst, The, 2014, 139, 3174-3178.	3.5	20
62	Junction Plasmon-Induced Molecular Reorientation. Journal of Physical Chemistry Letters, 2013, 4, 3435-3439.	4.6	22
63	Electrocatalytic properties of poly(3,4-ethylenedioxythiophene) (PEDOT) in Li-O2 battery. Electrochemistry Communications, 2013, 29, 63-66.	4.7	36
64	Enzyme-Directed Assembly of Nanoparticles in Tumors Monitored by <i>in Vivo</i> Whole Animal Imaging and <i>ex Vivo</i> Super-Resolution Fluorescence Imaging. Journal of the American Chemical Society, 2013, 135, 18710-18713.	13.7	104
65	Spatial and temporal variation of surface-enhanced Raman scattering at Ag nanowires in aqueous solution. Physical Chemistry Chemical Physics, 2013, 15, 850-859.	2.8	15
66	Raman Scattering at Plasmonic Junctions Shorted by Conductive Molecular Bridges. Nano Letters, 2013, 13, 1858-1861.	9.1	62
67	Potential of Nanocrystalline Cellulose–Fibrin Nanocomposites for Artificial Vascular Graft Applications. Biomacromolecules, 2013, 14, 1063-1071.	5.4	90
68	In Situ Live Cell Sensing of Multiple Nucleotides Exploiting DNA/RNA Aptamers and Graphene Oxide Nanosheets. Analytical Chemistry, 2013, 85, 6775-6782.	6.5	189
69	Understanding super-resolution nanoscopy and its biological applications in cell imaging. Physical Chemistry Chemical Physics, 2013, 15, 14856.	2.8	6
70	Role of Collector Alternating Charged Patches on Transport of <i>Cryptosporidium parvum</i> Oocysts in a Patchwise Charged Heterogeneous Micromodel. Environmental Science & Technology, 2013, 47, 2670-2678.	10.0	17
71	The Origin of Surface-Enhanced Raman Scattering of 4,4′-Biphenyldicarboxylate on Silver Substrates. Journal of Physical Chemistry C, 2013, 117, 7260-7268.	3.1	8
72	Coexistence of weak ferromagnetism and polar lattice distortion in epitaxial NiTiO3 thin films of the LiNbO3-type structure. Journal of Vacuum Science and Technology B:Nanotechnology and Microelectronics, 2013, 31, 030603.	1.2	17

ДЕНОИД НИ

#	Article	IF	CITATIONS
73	Delivery of MicroRNA-10b with Polylysine Nanoparticles for Inhibition of Breast Cancer Cell Wound Healing. Breast Cancer: Basic and Clinical Research, 2012, 6, BCBCR.S8513.	1.1	37
74	Factors affecting the battery performance of anthraquinone-based organic cathode materials. Journal of Materials Chemistry, 2012, 22, 4032.	6.7	126
75	Effects of cell positive cans and separators on the performance of high-voltage Li-ion batteries. Journal of Power Sources, 2012, 213, 160-168.	7.8	44
76	Super-resolution fluorescence nanoscopy applied to imaging core–shell photoswitching nanoparticles and their self-assemblies. Chemical Communications, 2011, 47, 1258-1260.	4.1	51
77	Photoswitchable Nanoprobes Offer Unlimited Brightness in Frequency-Domain Imaging. Journal of the American Chemical Society, 2011, 133, 7628-7631.	13.7	33
78	Reaction mechanisms for the limited reversibility of Li–O2 chemistry in organic carbonate electrolytes. Journal of Power Sources, 2011, 196, 9631-9639.	7.8	198
79	Investigation on the charging process of Li2O2-based air electrodes in Li–O2 batteries with organic carbonate electrolytes. Journal of Power Sources, 2011, 196, 3894-3899.	7.8	229
80	Investigation of the rechargeability of Li–O2 batteries in non-aqueous electrolyte. Journal of Power Sources, 2011, 196, 5674-5678.	7.8	197
81	Catalyst Structure-Performance Relationship Identified by High-Throughput Operando Method: New Insight for Silica-Supported Vanadium Oxide for Methanol Oxidation. Topics in Catalysis, 2010, 53, 40-48.	2.8	4
82	Nanometer resolution imaging by single molecule switching. Nano Reviews, 2010, 1, 5122.	3.7	2
83	Aptamer/Graphene Oxide Nanocomplex for <i>in Situ</i> Molecular Probing in Living Cells. Journal of the American Chemical Society, 2010, 132, 9274-9276.	13.7	1,020
84	Ternary Self-Assembly of Ordered Metal Oxideâ^'Graphene Nanocomposites for Electrochemical Energy Storage. ACS Nano, 2010, 4, 1587-1595.	14.6	795
85	Methanol Partial Oxidation on MoO3/SiO2 Catalysts: Application of Vibrational Spectroscopic Imaging Techniques in a High Throughput Operando Reactor. Topics in Catalysis, 2009, 52, 1381-1387.	2.8	14
86	Self-Assembled TiO ₂ –Graphene Hybrid Nanostructures for Enhanced Li-Ion Insertion. ACS Nano, 2009, 3, 907-914.	14.6	1,596
87	Clay Nanoparticle-Supported Single-Molecule Fluorescence Spectroelectrochemistry. Nano Letters, 2009, 9, 655-658.	9.1	52
88	Single-Molecule Electron Transfer Reaction in Nanomaterials. Microscopy and Microanalysis, 2009, 15, 1138-1139.	0.4	0
89	Single-molecule fluorescence spectroelectrochemistry of cresyl violet. Chemical Communications, 2008, , 5490.	4.1	77
90	Photoswitchable Nanoparticles Enable High-Resolution Cell Imaging: PULSAR Microscopy. Journal of the American Chemical Society, 2008, 130, 15279-15281.	13.7	105

Dеномс Hu

#	Article	IF	CITATIONS
91	High throughputoperandostudies using Fourier transform infrared imaging and Raman spectroscopy. Review of Scientific Instruments, 2008, 79, 074101.	1.3	16
92	Fluctuating Two-State Light Harvesting in a Photosynthetic Membraneâ€. Journal of Physical Chemistry C, 2007, 111, 8948-8956.	3.1	14
93	Submicrometer and Nanoscale Inorganic Particles Exploit the Actin Machinery To Be Propelled along Microvilli-like Structures into Alveolar Cells. ACS Nano, 2007, 1, 463-475.	14.6	42
94	Revealing Two-State Proteinâ^'Protein Interactions of Calmodulin by Single-Molecule Spectroscopy. Journal of the American Chemical Society, 2006, 128, 10034-10042.	13.7	69
95	Single molecule electron transfer process of ruthenium complexes. , 2006, , .		0
96	Tip-enhanced near-field Raman spectroscopy probing single dye-sensitized TiO2 nanoparticles. Applied Physics Letters, 2006, 88, 093121.	3.3	30
97	Single-Molecule Triplet-State Photon Antibunching at Room Temperature. Journal of Physical Chemistry B, 2005, 109, 9861-9864.	2.6	17
98	Probing Inhomogeneous Vibrational Reorganization Energy Barriers of Interfacial Electron Transfer. Journal of Physical Chemistry B, 2005, 109, 16390-16395.	2.6	29
99	Cholesterol Dictates the Freedom of EGF Receptors and HER2 in the Plane of the Membrane. Biophysical Journal, 2005, 89, 1362-1373.	0.5	116
100	Probing nanosecond protein motions of calmodulin by single-molecule fluorescence anisotropy. Applied Physics Letters, 2004, 85, 2420-2422.	3.3	29
101	Correlated topographic and spectroscopic imaging by combined atomic force microscopy and optical microscopy. Journal of Luminescence, 2004, 107, 4-12.	3.1	15
102	Correlated atomic force microscopy and fluorescence lifetime imaging of live bacterial cells. Colloids and Surfaces B: Biointerfaces, 2004, 34, 205-212.	5.0	56
103	Single-Molecule Study of Proteinâ^'Protein Interaction Dynamics in a Cell Signaling System. Journal of Physical Chemistry B, 2004, 108, 737-744.	2.6	51
104	Intermittent Single-Molecule Interfacial Electron Transfer Dynamics. Journal of the American Chemical Society, 2004, 126, 9374-9381.	13.7	102
105	Placing Single-Molecule T4 Lysozyme Enzymes on a Bacterial Cell Surface: Toward Probing Single-Molecule Enzymatic Reaction in Living Cells. Biophysical Journal, 2004, 87, 656-661.	0.5	33
106	FRET measurements between small numbers of molecules identifies subtle changes in receptor interactions. , 2004, , .		0
107	Single-Molecule Nanosecond Anisotropy Dynamics of Tethered Protein Motions. Journal of Physical Chemistry B, 2003, 107, 618-626.	2.6	42
108	Probing Single-Molecule T4 Lysozyme Conformational Dynamics by Intramolecular Fluorescence Energy Transfer. Journal of Physical Chemistry B, 2003, 107, 7947-7956.	2.6	92

ДЕНОИД НИ

#	ARTICLE	IF	CITATIONS
109	Correlated topographic and spectroscopic imaging beyond diffraction limit by atomic force microscopy metallic tip-enhanced near-field fluorescence lifetime microscopy. Review of Scientific Instruments, 2003, 74, 3347-3355.	1.3	46
110	Spatial Confinement of Exciton Transfer and the Role of Conformational Order in Organic Nanoparticles. Nano Letters, 2002, 2, 1121-1124.	9.1	73
111	Structural and Electronic Characterization of Chemical and Conformational Defects in Conjugated Polymers. Journal of Physical Chemistry B, 2001, 105, 6103-6107.	2.6	72
112	Collapse of stiff conjugated polymers with chemical defects into ordered, cylindrical conformations. Nature, 2000, 405, 1030-1033.	27.8	433
113	Unmasking Electronic Energy Transfer of Conjugated Polymers by Suppression of O2 Quenching. Science, 2000, 289, 1327-1330.	12.6	356
114	Single-Molecule Spectroscopy of the Conjugated Polymer MEH-PPV. Journal of the American Chemical Society, 1999, 121, 6936-6937.	13.7	162
115	Classifying the Photophysical Dynamics of Single- and Multiple-Chromophoric Molecules by Single Molecule Spectroscopy. Journal of Physical Chemistry A, 1998, 102, 7564-7575.	2.5	281
116	First Observation of the Key Intermediate in the "Light-Switch―Mechanism of [Ru(phen)2dppz]2+. Journal of the American Chemical Society, 1997, 119, 11458-11467.	13.7	370
117	Quantitative Modeling of DNA-Mediated Electron Transfer between Metallointercalators. Journal of Physical Chemistry B, 1997, 101, 299-303.	2.6	76
118	Discrete Intensity Jumps and Intramolecular Electronic Energy Transfer in the Spectroscopy of Single Conjugated Polymer Molecules. Science, 1997, 277, 1074-1077.	12.6	508